Polymer Chemistry

Accepted Manuscript

This is an *Accepted Manuscript*, which has been through the Royal Society of Chemistry peer review process and has been accepted for publication.

Accepted Manuscripts are published online shortly after acceptance, before technical editing, formatting and proof reading. Using this free service, authors can make their results available to the community, in citable form, before we publish the edited article. We will replace this *Accepted Manuscript* with the edited and formatted *Advance Article* as soon as it is available.

You can find more information about *Accepted Manuscripts* in the Information for Authors.

Please note that technical editing may introduce minor changes to the text and/or graphics, which may alter content. The journal's standard Terms & Conditions and the Ethical guidelines still apply. In no event shall the Royal Society of Chemistry be held responsible for any errors or omissions in this *Accepted Manuscript* or any consequences arising from the use of any information it contains.

ROYAL SOCIETY OF CHEMISTRY

www.rsc.org/polymers

Polymer Chemistry

RSCPublishing

PAPER

Quantifying bacterial adhesion on antifouling polymer brushes via Single-Cell Force Spectroscopy

C ite this: DOI: 10.1039/x0xx00000x

Received ooth,
Accepted ooth

DOI: 10.1039/x0xx00000x

www.rsc.org/

Cesar Rodriguez-Emmenegger,[a,*] Sébastien Janel,[b] Andres de los Santos Pereira,[a] Michael Bruns,[c] and Frank Lafont[b]

Bacterial adhesion poses serious problems in food safety and biomedical applications. Antifouling polymer brushes have been shown to be effective as surface modifications to prevent biofilm formation from pathogenic bacteria. In this work, the adhesion of *Yersinia pseudotuberculosis* on seven types of brushes is examined by Single-Cell Force Spectroscopy. The brushes, known to possess excellent resistance to protein adsorption, greatly reduced the maximum force and the work required to detach the bacterium.

Introduction

The adhesion and proliferation of bacteria on various types of surfaces constitutes a significant challenge in various industrial applications as well as in food safety and medicine, being the cause of adverse outcomes ranging from economic losses to severe disease and loss of life.[1-5] Among the most common problems observed are the biofouling of metallic components leading to the acceleration of their corrosion,[6] food-borne diseases caused by the unnoticed presence of pathogens in foodstuffs, and nosocomial infections.[2-5] In particular the surface of implantable medical devices is susceptible to colonisation, leading to recurrent infections. The ability of bacteria to adhere is considered an important factor in their virulence.[7] Once bacteria are attached to a surface, a series of processes is set in motion, which results in an adhering microbial community termed biofilm. The biofilm is an accumulation of bacterial cells on a solid surface, embedded in a matrix of excreted extracellular polymeric substances (EPS).[8] Such bacterial communities are largely protected from the immune response and much less susceptible to elimination by antibiotics, therefore increasing the detrimental consequences of the infection. Furthermore, sessile bacteria in the biofilm release antigens stimulating the production of antibodies. The latter are not effective in targeting bacteria in the biofilm and may result in the immune system damaging surrounding tissues. [9, 10] Consequently, the inhibition of bacterial colonisation of surfaces and the prevention of biofilm formation are a primary research focus.

The underlying processes leading to the formation of biofilms are common even across the variety of different environments in which they occur, with the concomitant differences in the resulting structure. Upon contact of a surface with a medium in which bacteria are present, the first step in the formation of a biofilm is the adsorption of biomacromolecules from the medium. This results in the generation of a layer that acts as a conditioning film. The transport of the bacteria to the substrate comes next, leading to adhesion upon contact of the bacterium with the surface.[7, 11] The synthesis of the biofilm matrix follows, as the attached

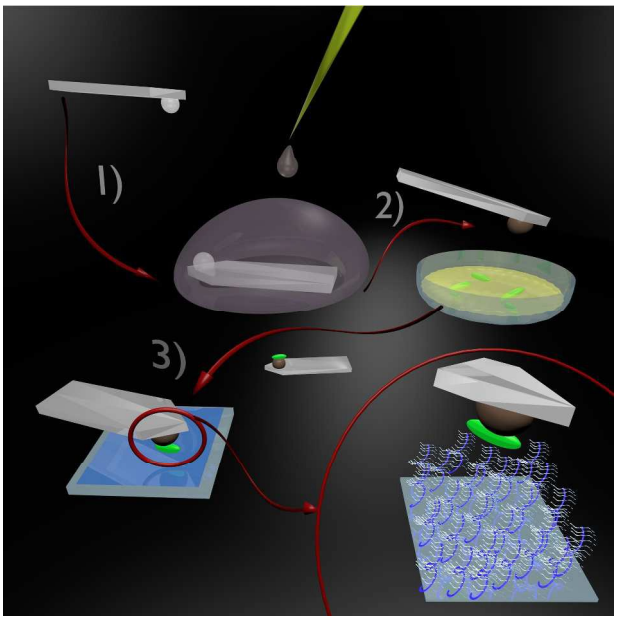

Fig. 1 Schematic representation of the immobilization of a single bacterium onto the colloidal tip cantilever. 1) Coating of the colloidal tip cantilever with a poly(dopamine) adhesion layer, 2) immobilization of a single bacterium on the colloidal probe, and 3) Single-cell force spectroscopy measurements.

bacteria activate the cellular mechanisms for the secretion of EPS. This creates an environment in which the bacteria benefit from improved mechanical stability and protection from adverse chemical conditions.[1, 7] Therefore, the eradication of the bacteria becomes significantly more challenging once this state has been achieved. Consequently, the formation of the biofilm needs to be prevented by appropriate coatings that will stop the process before the bacteria can be shielded. The process of bacterial colonisation and biofilm formation is further complicated by the complexity and the interplay of both the material and bacteria surfaces.[12]

Two general strategies have been employed for the prevention of biofilm formation based on (a) inactivating any bacterial cells which come into contact with the surface (bactericidal coating) and (b) avoidance of bacterial adhesion (antifouling). Interestingly, coatings combining both approaches have also been introduced.[13-16] Bactericidal coatings are based on molecules, polymers or nanoparticles which are toxic for the bacteria.[5, 17-23] Nevertheless, their intrinsic cytotoxicity is usually an impediment for their use in biomedical applications.[24, 25] Furthermore, the adsorption of the bacterium after inactivation leads to reduced effectiveness of the coating, as it can serve as an anchoring point for more bacteria to attach.[12] On the other hand an ideal non-fouling coating should prevent the formation of the conditioning film as well as the bacterial attachment. The inhibition of the conditioning film formation requires coatings able to prevent the adsorption of biomacromolecules, mainly proteins, while the bacterial adhesion can be prevented by minimising the forces driving the bacteria into contact with the surface.

The adhesion of bacteria onto hydrophobic surfaces is promoted by the conditioning film through a decrease in the interfacial energy when such surfaces come into contact with media containing proteins.[26-28] On the other hand, the factors determining the adhesion of bacteria onto hydrophilic surfaces can be separated into specific interactions by receptors on the bacterium surface (mainly adhesins) and general physicochemical interactions.[29] Long-range interactions are responsible for the initial adhesion and have been modelled by the extended Derjaguin-Landau-Verwey-Overbeek (DLVO) theory, considering the bacterial cell as a simple colloid. Moreover, the conformation of polymers grafted to the surface has been incorporated in the models.[30-32] The interaction is caused by the Liftshitz-Van der Waals forces and forces originating from the overlap of the electrical double layers.[32] The surface chemistry also plays an important role, as it determines the interactions operating in the short range (few nm), including electrostatic interactions as well as the formation of hydrogen bonds, and in a longer range (typically 5-10 nm) through hydrophobic attraction. Thus, the control of these interactions and the suppression of attractive forces are central to the prevention of bacterial adhesion and precluding the formation of a biofilm.

According to the extended DLVO theory attractive long-range interactions are minimised by introduction of a water barrier with a zero net charge and steric hindrance to keep the bacterial cell at a distance from the surface.[32, 33] For this purpose the grafting of poly(ethylene glycol) chains (PEG) to a surface and the formation of self-assembled monolayers of alkanethiols presenting oligo(ethylene glycol) head groups have been presented as coatings capable of limiting the fouling.[2, 34] The success achieved with these approaches is limited.[35, 36] PEG coatings typically reach only low thicknesses, while high grafting densities were accessible only when the achieved thickness was lower than about 10 nm, not sufficient to ensure a steric barrier.[32, 37-40] Furthermore, when exposed to media containing biological components, the ensuing adsorption could lead to a conditioning film promoting bacterial attachment.[26, 28, 41] Improved resistance to fouling was expected from coatings presenting more densely grafted, longer polymer chains on the basis of a more effective steric barrier combined with a higher surface coverage, less prone to defects.[38, 40, 42]

On the other hand, the "grafted-from" approach has been employed to grow polymer brushes by reversible-deactivation radical polymerisation methods, including atom transfer radical polymerisation (ATRP),[43] reversible addition fragmentation transfer (RAFT) polymerisation,[44] and single electron transfer radical polymerisation (SET-LRP).[45] The polymer layers obtained in this way from PEG-like monomer oligo(ethylene glycol) methacrylate, zwitterionic carboxybetaines, and *N*-(2-hydroxypropyl)methacrylamide (HPMA) have shown an unmatched resistance to the non-specific adsorption from human blood, plasma and other biofluids with which an implant could come into contact.[26, 46, 47] Moreover, hydrophilic brushes based on sulfobetaine methacrylate, carboxybetaines, and HPMA among others effectively prevented the formation of biofilms.[48, 49] Nevertheless, while the bacterial adhesion and the formation of biofilms can be assessed on a macroscopic scale by well-established techniques, these methods do not provide access to the fundamental forces responsible for the bacterial adhesion. On the other hand, due to the complexity of the process and the variety of factors involved, it is desirable to gain insight into the parameters governing the interactions of microbial cells and surfaces at a micro- and even nanoscopic scale. Fulfilling this need, recently a number of methods have emerged which allow to follow the forces occurring between a single cell and a solid surface. Three types of Single-Cell Force Spectroscopy (SCFS) assays have been developed based on micropipettes, optical or magnetic tweezers and Atomic Force Microscopy (AFM).[50-52] Of these techniques the AFM-based approach allows for the widest force range.[50] Via this technique a single bacterium can be attached to an AFM cantilever that is then approached to the tested surfaces to measure the adhesion force.[53-55] AFM-based SCFS enabled to assess the driving forces of various bacteria into common substrates as well as to recognise specific surface components that mediated bacteria adhesion to surfaces or even eukaryotic cells and helped to understand the process of infection.[50, 56-58] Therefore, this technique has a great potential to unravel the mechanisms by which antifouling polymer brushes are able to repel bacteria and prevent their adhesion. Pioneering studies showed moderate interactions of *Pseudomonas aeruginosa* on end-

grafted PEO which were modelled using DLVO theory.[32] Unfortunately, these brushes display only limited resistance to protein and bacteria adhesion.[28, 59]

In the present study we examine the forces involved in the adhesion of *Yersinia pseudotuberculosis*, a common pathogen, to seven types of state-of-the-art antifouling polymer brushes by SCFS. The brushes were selected on the basis of their resistance to protein adsorption as well as to reduce or prevent biofilm formation. The polymer were grafted by surface initiated atom transfer radical polymerisation. We aim to observe to which extent the antifouling properties towards proteins and complex biological media of the surfaces have an impact on the adhesion parameters of a bacterial cell. Making use of this technique, we aim to qualitatively correlate the chemical and physicochemical properties of the different polymer brushes to the strength of the adhesion of a single bacterial cell to the surface.

Materials and methods

All reagents employed for the preparation of the surfaces were acquired from Sigma-Aldrich, SERVA Electrophoresis, or synthesised according to literature procedures.[27] A detailed description can be found in the ESI.

The substrates employed for the SCFS experiments were borosilicate glass microscopy cover slips (thickness *ca.* 150 µm). For the chemical characterisation of the polymer brushes, the same sample preparation procedure was performed in parallel on microscopy glass slides, which were used for XPS measurements, and on silicon wafer chips for the ellipsometric determination of the dry layer thickness.

For the AFM experiments uniform glass microspheres of nominal diameter 10 µm were obtained from Structure Probe, Inc. (SPI), TL-CONT tipless cantilevers (nominal spring constant 0.2 N m^{-1}) were acquired from Nanosensors, and Biolever mini (k = 0.1 N m^{-1} nominal) cantilevers (topography) were purchased from Olympus.

Preparation of the surfaces

Immobilisation of silane-ATRP-initiator monolayer. The substrates were cleaned by rinsing twice with ethanol and deionised water, blown dry with nitrogen, and activated by air plasma cleaning for 20 min. Without delay they were placed in a solution of silane-ATRP-initiator (1 mg mL^{-1}, Fig. S2 in the ESI) in dry toluene and kept in a dry environment for 3 h. After removing the samples from the initiator solution, they were rinsed with toluene, acetone, ethanol, and deionised water, and blown dry with nitrogen.

Poly(HOEGMA). Ar was bubbled for 1 h while stirring a solution of oligo(ethylene glycol) methacrylate (HOEGMA, M_n = 500 g·mol^{-1}, 10 g, 20 mmol), $CuBr_2$ (8.1 mg, 36.4 µmol), and 2,2'-bipyridyl (145 mg, 930 µmol) in water (10 mL) to remove dissolved oxygen. CuCl (37 mg, 374 µmol) was added, dissolved under continued stirring, and the polymerisation solution was transferred to Ar-filled reactors containing the initiator-coated substrates. The reaction proceeded for 30 min at 30 ºC.

Poly(HEMA). Poly(2-hydroxyethyl methacrylate) (poly(HEMA)) brushes were prepared in analogous way as the brushes poly(HOEGMA), using as monomer HEMA (11.5 g, 89 mmol) and as solvent water/ethanol 1:1 (10 mL). The polymerisation proceeded for 40 min at 30 ºC.

Poly(MeOEGMA). The polymerisation of oligo(ethylene glycol) methyl ether methacrylate (MeOEGMA, M_n = 300 g·mol^{-1}) was performed as reported earlier.[60] In individual flasks, methanol, a solution of MeOEGMA (5.7 g, 19 mmol) in 5 mL of water, and a mixture of 2,2'-bipyridyl (155 mg,

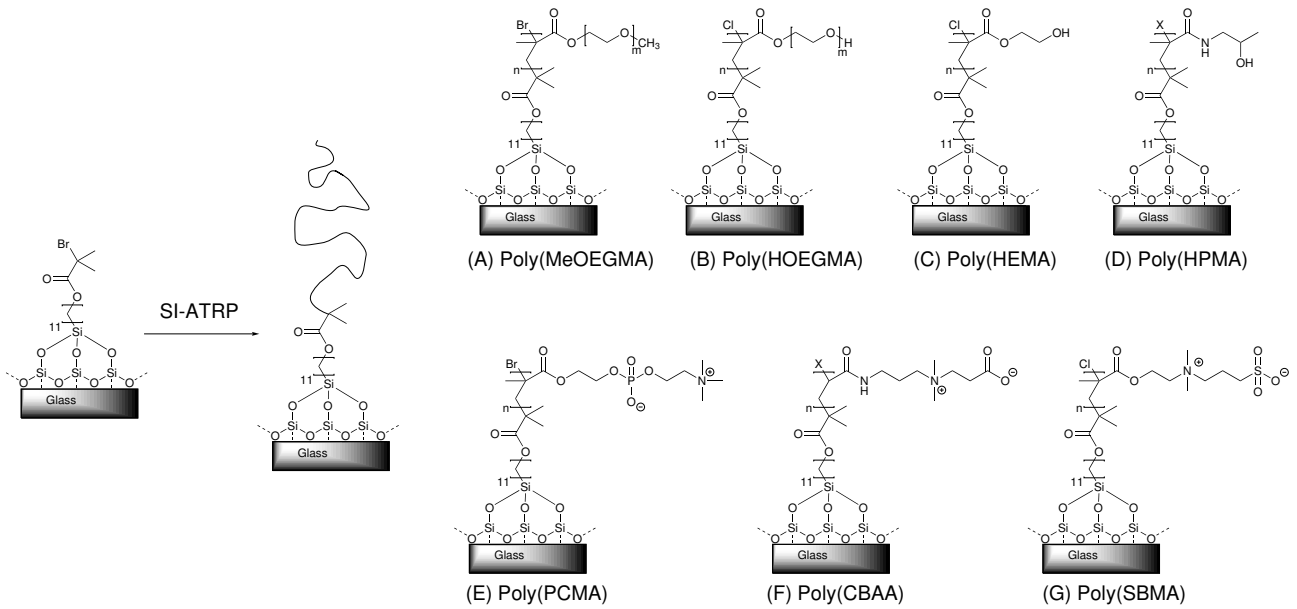

Scheme 1 Growth of antifouling polymer brushes by SI-ATRP from an immobilised SAM of initiator and chemical structures of the polymer brushes obtained, on which SCFS was performed.

991 µmol), $CuBr_2$ (16.8 mg, 75 µmol), and $CuBr_2$ (53.8 mg, 375 µmol) were degassed by bubbling with Ar for 1 h. Degassed methanol (5 mL) was transferred under Ar-protection to the mixture of solids, which were dissolved under stirring. Subsequently, the monomer solution was transferred to the flask containing the catalyst solution and they were mixed by stirring. The polymerisation solution was transferred to Ar-filled reactors containing the initiator-coated substrates. The reaction proceeded for 40 min at 30ºC.

Poly(HPMA). A mixture of methanol/water 9:1 was degassed by three freeze-pump-thaw cycles. In a Schlenk flask CuCl (14.8 mg, 149 µmol), $CuCl_2$ (4.4 mg, 33 µmol), and Me_4Cyclam (51 mg, 199 µmol) were degassed and 10 mL of the degassed solvent were added. The mixture was stirred until dissolution and the solution was transferred to a Schlenk flask containing degassed *N*-(2-hydroxypropyl) methacrylamide (HPMA, 1.18 g, 8.22 mmol). After dissolution, the polymerisation mixture was added to Ar-filled reactors containing the initiator-coated substrates and the reaction proceeded for 2 h at 30ºC.

Poly(PCMA). Polymer brushes of 2-methacryloyloxyethyl phosphorylcholine (PCMA) of the desired thickness were obtained by a modification of published protocols.[61, 62] In separate Schlenk flasks, PCMA (2.5 g, 8.48 mmol) and a mixture of $CuBr_2$ (9.5 mg, 43 µmol), CuBr (20.23 mg, 142 µmol), and 2,2'-bipyridyl (61.8 mg, 396 µmol) were degassed by pump/refill cycles with Ar. Water and methanol were separately degassed by Ar bubbling for 1 h. Subsequently, 5 mL of each solvent were transferred to the flask containing the catalyst components and they were dissolved under stirring. The catalyst solution was added to the flask containing the monomer and it was stirred until dissolution. The polymerisation mixture was transferred to the reactors containing the initiator-coated substrates and the reaction proceeded for 90 min at 30 ºC.

Poly(SBMA). Polymer brushes of [2-(methacryloyloxy)ethyl]dimethyl-(3-sulfopropyl)ammonium hydroxide (SBMA) of the desired thickness were obtained by a modification of published protocols.[63] In separate Schlenk flasks SBMA (3.75 g, 13.4 mmol) and a mixture of $CuCl_2$ (7.3 mg, 54 µmol), CuCl (26.7 mg, 270 µmol), and 2,2'-bipyridyl (105.4 mg, 675 µmol) were degassed by pump/refill cycles with Ar. Water and methanol were degassed by Ar bubbling for 1 h. Degassed methanol (8 mL) and water (2 mL) were transferred under Ar-protection to the flask containing the catalyst mixture, which was stirred until dissolution. The catalyst solution was transferred to the flask containing the monomer and it was stirred until dissolution. The polymerisation mixture was transferred to Ar-filled reactors containing the initiator-coated substrates and the reaction proceeded for 1 h at 30 ºC.

Poly(CBAA). Polymer brushes of (3-acryloylamino-propyl)-(2-carboxyethyl)-dimethyl-ammonium (CBAA) were obtained by a protocol published earlier.[64] PBS (10 mL) was degassed by three cycles of freeze-pump-thaw and transferred under Ar protection to a Schlenk flask containing CuBr (19.1 mg, 133 µmol), $CuBr_2$ (5.9 mg, 26.5 µmol), and Me_4Cyclam (40.9 mg, 160 µmol), previously degassed by pump/refill with Ar. The solids were dissolved by stirring and the catalyst solution was transferred to a Schlenk flask containing the CBAA monomer (1.5 g, 6.7 mmol) and stirred. The polymerisation solution was transferred to Ar-filled reactors containing the initiator-coated substrates. The reaction proceeded for 2 h at 30ºC.

In all cases the polymerisations were stopped by removing the substrates and rinsing them first with water, then ethanol, and finally water. The samples were kept in water until they were used for further experiments.

Physico-chemical characterisation

The thickness, chemical composition and wettability surfaces were characterised by ellipsometry, X-Ray photoelectron spectroscopy (XPS), and dynamic water contact angle, respectively, while the protein fouling quantified by surface plasmon resonance spectroscopy (SPR). Detailed experimental procedures can be found in the ESI.

Atomic Force Microscopy

Topography experiments. Topography images of the brushes in phosphate buffered saline (PBS, pH 7.4) were acquired with a JPK NanoWizard III Ultra mounted on an Olympus IX83 inverted microscope using JPK BioCell. The BioCell enables to perform the measurement of brushes in the swollen state (PBS) at a controlled temperature of 37 °C. The surfaces were scanned using an Olympus Biolever mini cantilever ($k = 0.1$ N m^{-1} nominal) in the QI mode. The spring constant of the cantilevers was calibrated first by performing a force distance curve in a hard material and then by the thermal noise method using a Lorentzian fit. The acquisition parameters employed were: 800 nm ramp, tip velocity 30 µm s^{-1} and a force trigger of 200 pN over a surface of 10 µm^2 (128x128 pixel). Each force curve was analysed to determine the point of contact thus allowing to access the zero force image.

Bacteria culture. *Yersinia pseudotuberculosis* strain IP32777 expressing the isopropyl-β-D-thiogalactopyranoside (IPTG)-inducible GFP was constructed as described elsewhere[65] and cultured overnight in a Luria Bertani broth with ampicillin (100 µg mL^{-1}). Plasmid p67GFP3.1 (a pMMB67EH derivative harbouring the IPTG-inducible GFP-encoding gene) was kindly provided by J. Bliska (Stony Brook University, NY, USA). A 1/100 dilution fresh culture was started the following morning. When the bacteria reached the exponential growth phase (as measured by the OD_{600}) fluorescence was induced with isopropyl β-D-1-thiogalactopyranoside (IPTG, 3 mM). Subsequently 1 mL of the culture was deposited on a glass Petri dish for 10 min. The dish was then gently rinsed with pre-warmed PBS and transferred to the microscope stage equipped with an incubation chamber at 28 °C.

Preparation of the colloidal probe AFM cantilever. A custom made ball-tip cantilever was used for the SCFS studies. A detailed procedure of its preparation can be found in the ESI.

The colloidal probe cantilever was cleaned with O_2-plasma (Diener Electronic Femto 50% power, 15 min) and then immersed for 1 h in a 4 mg mL^{-1} dopamine hydrochloride solution in TRIS buffer, pH 8.5 (Fig. 1). This leads to the formation of a poly(dopamine) (PDA) film which can be subsequently exploited as a bioinspired wet adhesive to fix a bacterium to the cantilever (see below). The PDA-coated colloidal probe cantilever was installed in a Bruker BioScope Catalyst instrument mounted on an inverted fluorescence Zeiss AxioVert 200m microscope in an S2 security lab. The spring constant was calibrated using the thermal noise method provided by the Bruker NanoScope software.

Attachment of a single bacterium to the colloidal probe. The cantilever was approached toward a single bacterium with visual control using the video microscope (100x objective) and force control of the AFM. The contact was established for 30 s with a force smaller than 1 nN. The cantilever was then withdrawn with the bacterium attached. We then screened the surfaces using the same bacterium. At the end of the experiment we checked that the bacterium was still alive through its emission of fluorescence.

Single cell force spectroscopy. SCFS measurements were performed in PBS at 28 ºC using a Bioscope Catalyst AFM. Multiple force curves were recorded on various spots of the surfaces using a maximum applied force of 1 nN, a contact time of 1 s, a constant approach and retraction velocity of 6 µm s^{-1}, and a ramp size of 3 µm. The curves were acquired with the Z closed loop ON. Data were then automatically analysed using in-house developed software (pyAF: python Atomic Force) for detection and analysis of adhesion events (position on the retraction curve, force value and number of events), detachment force (maximum negative force) and adhesion work (area above the retraction curve). Boxplots were plotted with BoxPlotR software.[66]

Results and discussion

Polymer brushes synthesis and physico-chemical characterisation.

In the current study the interaction of *Yersinia pseudoturberculosis* with highly protein resistant polymer brushes was assessed. Firstly, a self-assembled monolayer (SAM) of a silane initiator was formed on the surface of the freshly activated glass substrates (Figure S3 in the ESI). The formation of this layer was clearly evidenced by the high resolution C1s and Br3d XPS spectra (Fig. S3 in the ESI) as well as for a marked increase in the water contact angle from 7º (clean glass) to 81º (SAM) as shown in Table 1. The thickness of the surface modifications was measured on the surface of silicon wafer chips prepared in parallel with the glass surfaces. The thickness of the layer was found to be 1.2 nm by ellipsometry (Table 1). This thickness is in agreement with the molecular dimensions of the initiator and the formation of a well-defined monolayer.

Table 1 Contact angles and ellipsometric thickness of the surfaces

Surface	Dry thickness [nm][a]	Water contact angle [°]	
		Advancing	Receding
Glass	-	7±1	-[b]
Initiator SAM	1.2±0.1	81±1	66±2
Poly(MeOEGMA	28.4±0.9	59±1	27±1
Poly(HOEGMA)	30.6±0.8	55±1	26±2
Poly(HEMA)	25.6±0.9	55±1	34±2
Poly(HPMA)	19.2±0.3	52±2	9±2
Poly(PCMA)	39.9±4.2	-[b]	-[b]
Poly(CBAA)	18.3±0.4	22±3	4±1
Poly(SBMA)	29.1±1.6	-[b]	-[b]

[a]: The dry thickness was determined on polymer brushes grafted from silicon wafer and is reported as the mean ± standard deviation from measurement on 3 random points of the surface.

[b]: The angle was too low to be measured (below 4 º) due to spreading of the drop.

The bromoisobutyrate groups were exploited as initiating sites for the SI-ATRP of seven polymer brushes (Scheme 1). The SI-ATRP of the methacrylate monomers has been shown to be highly versatile and well controlled, as evidenced by the linear evolution of the thickness with polymerisation time and the possibility to access multiblock copolymers with excellent resistance to fouling.[41, 67] On the other hand, the SI-ATRP of CBAA and HPMA shows the typical weak points of (meth)acrylamides –lack of control and livingness-,[27] but could be optimised to achieve the desired thickness.

The growth of polymer brushes was accompanied by a reduction in the dynamic water contact angles owing to the hydrophilic character of the polymer side chains (Table 1). The more pronounced decrease in the receding contact angles compared with the advancing contact angles can be explained by the strong interaction of the swollen polymer layers with water. The polymers presenting zwitterionic groups hydrate more strongly, resulting in the lowest water contact angles. Furthermore, ellipsometric measurement of the dry layer thickness confirms the growth of the polymer brushes. We targeted a thickness between 20-30 nm as this range has been shown to result in the best resistance to fouling.[27, 49, 68]

In-depth chemical characterisation of the brushes was carried out by XPS, confirming the expected chemical structures.[46] The high resolution scans of the C1s region of the spectra of all methacrylate polymer brushes (poly(MeOEGMA), poly(HOEGMA), poly(HEMA), poly(PCMA), and poly(SBMA)) show an ester peak at 289.0 eV (O-C=O). On the other hand poly(CBAA) and poly(HPMA), an acrylamide and a methacrylamide respectively, present an amide peak around 287.9 eV. The brushes containing oligo(ethylene glycol) lateral chains display a predominant C-O peak at 286.4 eV. In the case of poly(HEMA), this contribution is comparatively smaller due to the short side chain, but still visible. A signal arising from the tertiary carbon can be resolved at 285.9 eV for poly(HEMA) and both oligo(ethylene glycol) methacrylate brushes. For poly(HPMA) the peaks stemming from C-N and the tertiary

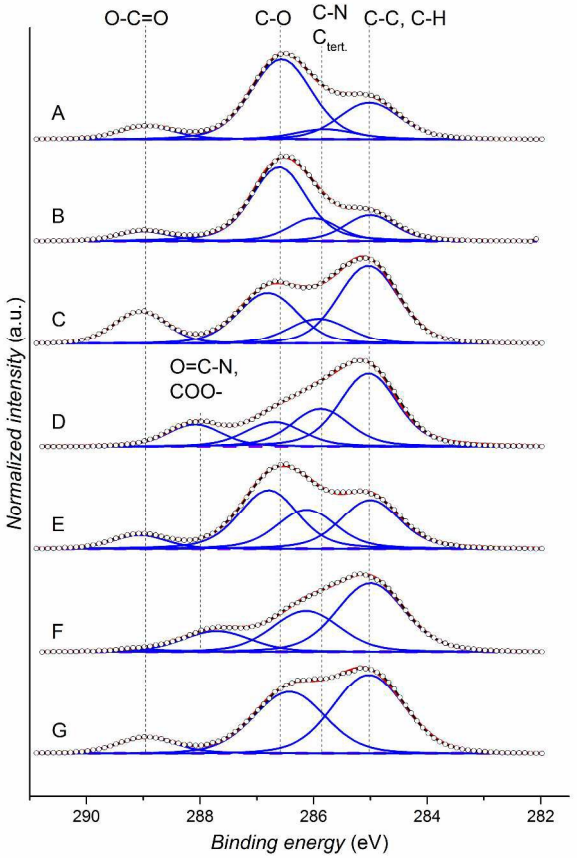

Fig. 2 High resolution XPS spectra of the C1s region of the polymer brushes: (A) poly(MeOEGMA), (B) poly(HOEGMA), (C) poly(HEMA), (D) poly(HPMA), (E) poly(PCMA), (F) poly(CBAA), and (G) poly(SBMA)

carbon from the methacrylamide appear overlapped at 285.9 eV while the C-O signal is also observed at 286.7 eV binding energy. The three zwitterionic polymer brushes show peaks for the C-N group arising from the quaternary ammonium groups. The presence of nitrogen, sulphur, and phosphorus is detected in the corresponding spectrum regions of the brushes in which these elements are expected. A detailed analysis of the N1s, P2p, and S2p regions as well as the measured and predicted relative atomic compositions can be found in Fig. S4 and Table S1 of the ESI.

The topography of the brushes swollen in PBS was accessed by AFM using the Quantitative Imaging mode (QI-mode, JPK instruments). In this mode a complete force-distance curve is made for each pixel and the point of contact –zero force- is determined, thus resolving the real topography. The commonly used contact or tapping mode, on the other hand may result in an altered topography as compressive and lateral forces are exerted on the surface, while having poor control over the vertical force. Examination of the topography images (Fig. S5 in the ESI) shows that the brushes form homogeneous films without pinholes. While bacteria could adhere to nanoscale flaws,[69] such defects could not be observed by AFM on the present brushes, even though the thickness of the brush would make their identification less accessible due to lateral collapse of the thick layer. Nevertheless, it is expected that this effect should also make the attachment of bacteria to tiny imperfections not seen by AFM –if present– less plausible. The roughness (R_q) of the brushes was below 7 nm except for those based on poly(PCMA), which displayed a marked increase in the roughness, suggesting some reorganisation of the chains (Fig. S5 in the ESI).

The protein fouling was evaluated by SPR on model brushes grown from a SAM of ω-mercaptoundecyl bromoisobutyrate on gold-coated glass SPR chips using a custom-made SPR system reported previously.[70] The model brushes were polymerised in parallel with those grown on glass. All brushes showed a remarkable resistance to the adsorption of human serum albumin (main plasma protein) as well as to fibrinogen, involved in the coagulation cascade (Table S2 in the ESI). A more challenging fluid was undiluted blood plasma. However, all brushes reduced the fouling at least by 92% compared to bare gold, being superior to other surface modifications such as end-grafted PEG or SAMs of ω-oligo(ethylene glycol) alkanethiols.[26, 59] The only exception to this behaviour were the brushes based on poly(PCMA) which were rapidly fouled by blood plasma, even though they prevented fouling from human serum albumin and fibrinogen. The high plasma fouling might be associated with the higher roughness (Fig. S5) observed on these brushes as described previously.[71, 72] It is also possible that some binding partner for the phosphorylcholine group, present in the highly complex blood-derived medium, could be attaching and is responsible for the fouling. Poly(HPMA) and poly(CBAA) displayed undetectable levels of fouling, thus being so far the only non-fouling brushes. The high (even total) suppression of fouling observed on these surfaces suggests that any adhesion of bacteria will be mediated directly by interactions with the substrate and not with a pre-adsorbed conditioning film of proteins. This is fundamental to avoid additional interactions with pre-adsorbed biomolecules while assessing the forces between the bacterium and the brushes.

Bacterial adhesion force

Prevention of bacterial adhesion on surfaces is of critical importance for medical devices and the food industry, among others. Usually, bacterial adhesion is mediated by the formation of a preconditioning film, which supports the subsequent adhesion of bacteria.[73-75] However, on antifouling polymer brushes, which inhibit the formation of the conditioning film, bacterial adhesion can still occur but mediated directly by the interaction of the bacterium surface with the material. Such interactions result from the interplay of Lifshitz-Van der Waals forces (always attractive), electrostatic forces, and hydrogen bonding.[7, 30, 32] Additionally bacteria can interact with surfaces by means of proteins on the surface called adhesins or through their pili.[76] Therefore the complex nature of the adhesion requires a technique able to directly assess the interaction forces between a living single bacterium and a surface to understand the parameters governing bacterial adhesion. The excellent control of force and position accessible by AFM results in unprecedented possibilities to directly quantify the

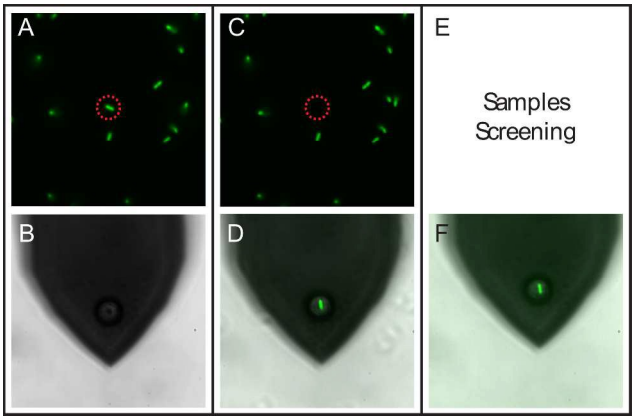

Fig. 3 Capture of a single bacterium on the polydopamine-coated colloidal probe cantilever. (A) Fluorescence image of the bacteria in the petri dish mounted on the AFM-inverted microscope,(B) optical image of the colloidal probe approaching the targeted bacterium, (C) remaining bacteria after capture and removal of the targeted cell by the colloidal probe, (D) combined optical/fluorescence microscopy image of the single bacterium attached to the colloidal probe, (E) acquisition of the F-d curves on the surfaces under study, and (F) observed fluorescence of the immobilised bacterium, still alive after the SCFS measurements.

interactions with a surface at the single cell level. The SCFS were conducted in PBS. The selection of this media without proteins allows the quantification of the forces of the bacterium with the surface without interferences from a conditioning film. Thus enabling to compare the forces observed on brushes –which prevent the formation of such film– with other surfaces such as glass, Teflon or PS which otherwise would be fouled by biomolecules. To probe the adhesion of *Y. pseudotuberculosis* on antifouling polymer brushes we utilised a recently developed protocol combining a colloidal probe cantilever with a bioinspired wet adhesive.[77] A colloidal probe cantilever was selected over a tipless one, since the former configuration affords better control of the cell-substrate interaction area and prevents the heating of the cell by the laser, which may cause bacterium death.[54] Colloidal probe cantilevers were produced by attaching a silica microsphere to a tipless cantilever (Fig. 3 B and S2 in the ESI). A highly adhesive PDA film was deposited in the cantilever by immersing it in a dopamine solution in TRIS buffer for 1 h.[78] Using an integrated AFM-inverted optical microscope the PDA-coated cantilever was approached to a single bacterium deposited in a petri dish in buffer (Fig. 3 A), kept in contact for 30 s and withdrawn (Fig. 3, C and D). The obtained bacterial probe was directly utilised for the SCFS measurements in PBS, although avoiding dewetting since this could lead to cell detachment or irreversible changes on the surface of the bacterium.

The success of SCFS can be hampered by the problems associated with the immobilisation of a single bacterium onto the cantilever –strength and position- as well as viability of the bacterium during the experiment. A firm immobilisation is crucial for the accurate evaluation of the force-distance curves.[56] Fig. 3 D and F showed that the bacterium was firmly immobilised in the centre of the colloidal probe and remained in the same place after probing all the surfaces.[77] It is worth noting that adhesion tests were performed with the same probe, therefore allowing comparison of the different surfaces in the most reliable way, mainly preventing bias coming from differences in the contact surface. The bacterium was still viable after all the tests as proven by the emission of fluorescence (Fig. 3 F) immediately after finishing the experiments. Furthermore, fluorescence images of the modified cantilever taken 20 h after SCFS experiments show that the bacterium was still able to divide thus unambiguously confirming the viability of the cell (Fig. S6 in the ESI).

Figure 4 A shows a typical de-adhesion force-distance retrace (F-d) curve in which a first phase describes the pulling with the concomitant increase in the force. The largest adhesion force, hereafter termed detachment force (F_D), represents the maximum force with which the bacterium binds to the surface. After the bacterium starts to detach, individual rupture events can be observed, associated with the adhesion of cell surface domains. The work required to completely separate the bacterium from the surface, a measurement of the strength of adhesion, was calculated as the integral of the F-d curve.

Representative F-d curves are displayed in Fig. 4 B and C. The general features of the curves did not substantially change when recording consecutive curves in different spots of the surface. Qualitatively, it can be observed that the curves obtained for the reference substrates as well as for the polymer brushes present similar features. However, the differences in the magnitude of the detachment force become evident when plotting the curves in the same scale (Fig. 4 C).

The adhesion of *Y. pseudotuberculosis* was assessed on glass as well as on PS and PTFE, typical materials usually found in food packaging and biomedical applications ranging from Petri dishes to catheters or stents. Interactions extending

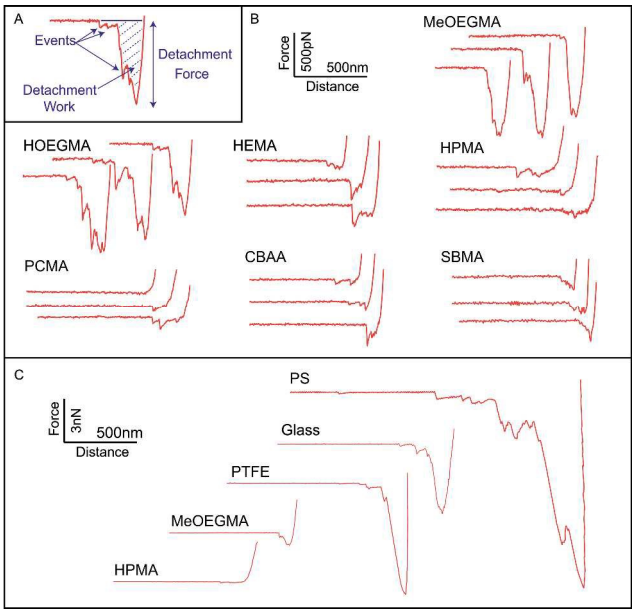

Fig. 4 Examples of force-distance curves measured on various surfaces. (A) Example showing the main parameters obtained. Representative curves on polymer brushes (B) and on unmodified glass, PS and PTFE compared to poly(MeOEGMA) and poly(HPMA) brushes (C)

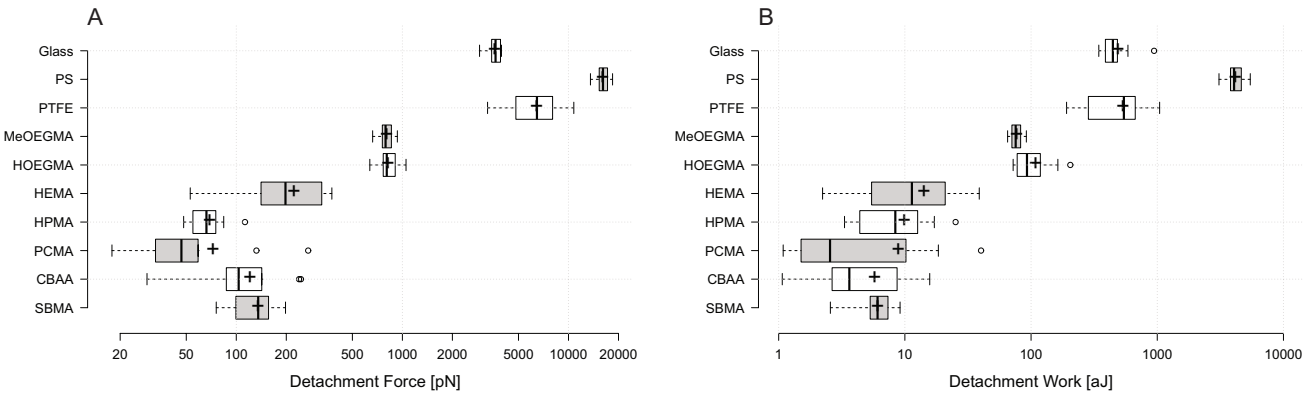

Fig. 5. Global parameters obtained from the force curves: detachment force (A) and detachment work (B). Centre lines represent the medians, box limits indicate the 25th and 75th percentiles as determined by R software, whiskers extend 1.5 times the interquartile range from the 25th and 75th percentiles, outliers are represented by circles and crossed represent the sample mean.

up to distances over 2 µm (Fig. 4) were observed on bare glass with F_D as high as 3600 pN (Fig. 5). Similar adhesion has been reported for other pathogens on glass previously, even if these values depend on the pulling speed of the cantilever. [54-56] PS and PTFE –usually regarded as non-adhesive by medical practitioners- showed even stronger interactions, characterised by F_D 16000 and 6500 pN, respectively and extended interaction distances up to 2 µm (Fig. 4 and 5). This can be associated with their hydrophobic nature.[56] On the other hand, the polymer brushes tested showed a markedly lower interaction with the *Y. pseudotuberculosis*. The observed median of the F_D for the brushes based on MeOEGMA and HOEGMA was less than 22% of the F_D observed on glass. The rest of brushes reduced the maximal force by no less than 95% (F_D 46-200 pN). It is worth noting that only few techniques can reliably measure the low forces observed on the tested brushes.[77] The weak forces observed on the brushes can be related with the physical barrier. All the presently studied brushes are hydrophilic, swollen chains with strong excluded volume interactions. The compression of the brushes by an incoming bacterium leads to increased osmotic pressure (repulsion) and a hydration pressure, thus minimising the short range forces (electrostatic, hydrogen bonding) and keeping the Lifshitz-Van der Waals forces relatively weak as the they decrease with increasing distance. Additionally, a high wettability reduces the Lifshitz-Van der Waals interactions. The theoretical conceptualisation is in line with the weak forces observed on highly wettable polyzwitterions but does not explain the comparatively low forces observed on poly(HPMA).

The decreases in the F_D as well as in the distance of the interactions were also reflected in the detachment work. The unprotected surfaces required a work of 450 and 550 aJ to detach the bacterium from glass and PTFE while 7000 aJ were necessary to separate the bacterium from the widely used PS. On the other hand, the polymer brushes reduced the work to unmatched figures (Fig. 5B).[32, 54, 79] Only 100 aJ were enough to detach the bacteria from the brushes based on oligo(ethylene glycol) methacrylates amounting an 80% reduction with respect to glass. This represents less than 3% of the work required for PS. The detachment work observed for these brushes was in the same order as in previously published reports using densely end-grafted PEO.[32] Moreover, a significantly lower work, less than 10 aJ, was necessary to separate the bacterium from the polyzwitterionic and poly(HPMA) brushes. This work represents less than 2% and 0.2% of the work necessary to detach the same bacterium from glass and PS respectively. Compared with other surface modifications studied by SCFS, the values of work obtained here are the lowest reported, showing the superiority of the brushes to prevent bacteria adhesion.[32, 55, 80] This is also in agreement with previous studies by conventional culturing methods.[49, 81]

The detachment of the bacterium from a surface can be broken down in a series of events, each representing the rupture of an individual association phenomenon (Fig. 6). Even though strong adhesion can hide some of the events, the number of events detected indicates the tendency of the bacterium to stay in contact with the surface. The number of rupture events observed in each F-d curve (median) on PS was as high as 12, while on glass and PTFE the number of events per curve was 8 and 5 respectively. Poly(HOEGMA) force curves displayed a median of 7 rupture events. Only 3 or less rupture events could be distinguished in all the remaining brushes. The force and distance were further extracted for each observed event (Fig. 6, B and C). The event force curve gives some information about the single bond strength, while the force-distance curve informs about the ability of the bacterium to detach upon minimal separation from the surface. While the event force for PS is markedly large (643 pN), the event force on glass was comparable to the one observed for poly(HOEGMA) and poly(MeOEGMA) brushes (110-130 pN). The more hydrophilic polyzwitterionic and poly(HPMA) brushes displayed considerably weaker event forces (25-65 pN). Interestingly, the higher roughness of PCMA did not lead to an increase in the forces as observed for proteins.

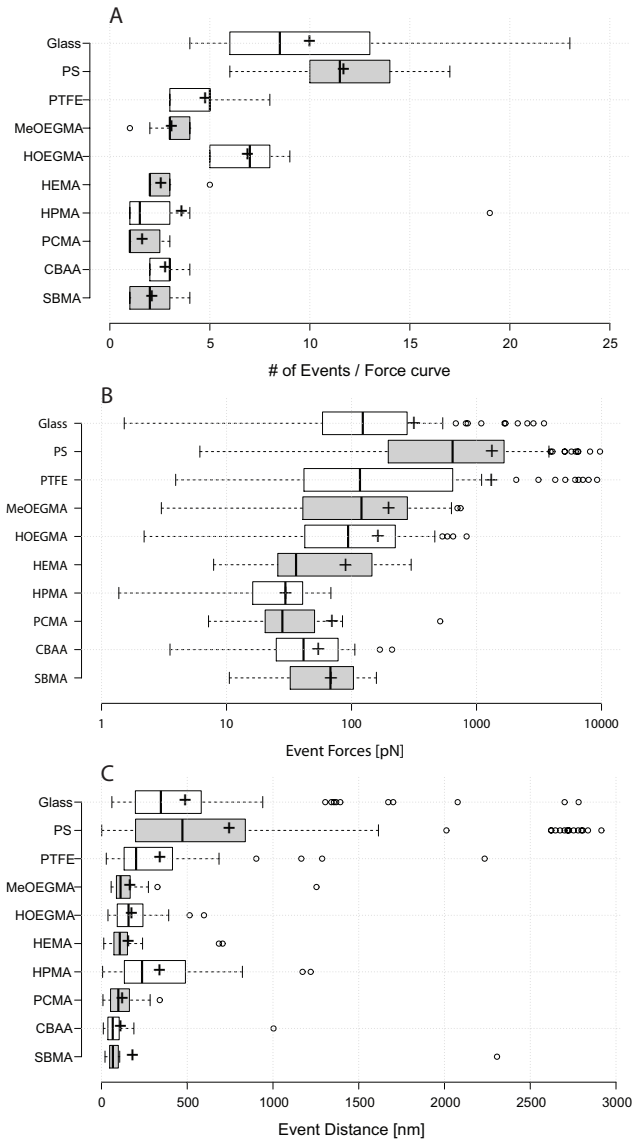

Fig. 6. Event parameters: (A) number of events per force curve, (B) force of a single rupture event, and (C) rupture event distance. Centre lines represent the medians, box limits indicate the 25th and 75th percentiles as determined by R software, whiskers extend 1.5 times the interquartile range from the 25th and 75th percentiles, outliers are represented by circles and crossed represent the sample mean.

Analysis of the event distance showed that the rupture event on the brushes occurred at shorter distances than on glass and PS. Surprisingly, the median of the event distance for poly(HPMA) brushes (240 nm) was out of line with the other brushes and close to that of glass (346 nm). However, the weaker forces exerted on poly(HPMA) brushes resulted in a lower overall detachment work. The rupture events for poly(HPMA) are spread out across a longer distance, but they represent the disappearance of a very small initial detachment force. Therefore, each event is associated with a minimal force, with a median of 29.5 pN and never exceeding 100 pN (Figure 6 B).

On the other hand, the capability of the bacterium to maintain the adhesion force to the surface even when being pulled over a certain distance appears to be critical for the high detachment work observed in the uncoated reference substrates. Even though PTFE displays an F_D almost twice as large as glass, the detachment work is very similar (Figure 5), which can be explained by the rupture events occurring at very short distances for PTFE, substantially lowering the adhesion work.

In the case of the polymer brushes, the same effect seems apparent, while even more pronounced. The occurrence of the bulk of the detachment events at short distances along the F-d curve is associated with a rapid drop in the remaining adhesion force between bacterium and surface. Moreover, the detachment force to be overcome in order to separate the bacterium from the surface is much lower for the polymer brushes, especially for poly(HPMA) and the polyzwitterions. In this way, the adhesion between the polymer brushes and the bacterium immobilised on the colloidal probe is substantially weaker, characterised by a markedly smaller detachment work.

It should be noted, that in the present study the bacterial adhesion was measured in a buffer in order to access the direct interaction of the bacterium with the surface. Nevertheless, the presence of preadsorbed biomolecules cannot be excluded when dealing with surfaces that suffer from fouling by complex biological media. Such conditioning layers are expected to dramatically alter the nature of bacteria-surface interactions, as the properties of the surface would be modified and bacterial outer proteins would play a major role. These phenomena have attracted considerable attention.[76] The adhesin YadA, expressed in *Yersinia pseudotuberculosis* at 37 ºC, is known to bind to collagen, fibronectin, and laminin as well as hydrophobic regions, being an important factor in its virulence.[82]

On antifouling polymer brushes, which prevent the adsorption of proteins and formation of the conditioning film, biofilm formation could still occur owing to the high complexity of the process.[12] It is therefore interesting to compare the trends of the bacterial adhesion parameters with the previously observed antifouling behaviour of similar brushes towards proteins and biofilm formation. Poly(HPMA) and poly(CBAA) are so far the most protein-resistant brushes available, outperforming all other polymer brushes in this respect.[27, 83] In the case of poly(CBAA), a strong hydration and organization of water at the interface have been proposed to explain this non-fouling behaviour.[81, 84, 85] In the case of poly(HPMA), the mechanism is so far less clear. Together with the remaining strongly hydrated polyzwitterions these brushes show the lowest detachment force and work. The oligo(ethylene glycol)-derived brushes show a lower reduction in the bacterial adhesion parameters observed by SCFS and a slightly worse resistance against protein fouling as well. It is particularly interesting to note that this correlation is observed even in the absence of a conditioning film. This suggests that the same physico-chemical mechanisms used to explain antifouling behaviour towards proteins may be at play in the direct interaction of the polymer brushes with the bacterium surface.

Remarkably, the comparison of the results obtained by SCFS with the ability of similar systems to prevent the

formation of biofilms during long-term experiments shows similar trends.[12, 48, 49] In light of the present results, it can be argued that both the inhibition of the formation of a conditioning film as well as the decrease in the strength of the direct adhesion observed in this study contribute to the prevention of biofilm formation previously reported for polymer brushes. Nevertheless, it should be kept in mind that the complexity of the process of bacterial adhesion and colonisation prevents it from being explained only by the formation of a conditioning film or the reduction of the detachment parameters. For example, the presence of surface defects could serve as anchoring points.

From a very general perspective, the nanoscale origin of the differences observed among the surfaces for the adhesion work, detachment force, and the distribution of the rupture events and their forces could be related to the interactions between the surfaces and the individual components of the cell. The remarkably low values obtained for the detachment work on the polymer brushes could then be explained by their well-established resistance to adsorption from biomolecules. In this regard, further SCFS with different types of bacteria including strains with specific protein knock down is needed since bacteria will respond to the substrate in different ways depending on their surface properties. Due to the complexity and interplay of the bacteria surface components, specifically targeted chemical force spectroscopy experiment could help shed light on the specific components and mechanisms involved in the adhesion of bacteria.

Conclusions

Seven antifouling polymer brushes were grown from glass via SI-ATRP and characterised by XPS, AFM, SPR and contact angle.

SCFS was introduced as a valuable approach to quantify the adhesive forces of a single bacterium on highly protein resistant brushes. The adhesion forces of *Y. pseudotuberculosis* on glass and other relevant substrates were characterised by large rupture forces in the range of several thousands of pN. On the other hand, the maximum force required to separate the bacterium from the brushes was reduced up to 99% and receded at shorter distances. Concomitantly, the work necessary to detach the bacterium from the brushes was between 2 and 20% of the work employed on glass. The polyzwitterionic brushes, showing the highest wettability, displayed the weakest interaction with the bacterium. This is in close agreement with the DLVO theory.

The results presented in this work highlight the potential of SCFS as a tool to understand the cause for the outstanding prevention of bacterial adhesion by the tested polymer brushes. Further studies should include different types of bacteria in order to investigate the influence of the different features present on the surface of bacterial cells.

Acknowledgements

We thank M. Popoff for his expertise with the pyAF software and N. Barois for the SEM images. This research was supported by the Grant Agency of the Czech Republic (GACR) under contract no. 15-09368Y, the COST Action AFM4NanoMed&Bio (TD 1002), and ANR-10-EQPX-04-01. The European Regional Development Funds is acknowledged for support under the project "BIOCEV – Biotechnology and Biomedicine Centre of the Academy of Sciences and Charles University" (CZ.1.05/1.1.00/02.0109), OPPK CZ.2.16/3.1.00/21545 and 12001407.

Notes and references

[a] Institute of Macromolecular Chemistry, Academy of Sciences of the Czech Republic, v.v.i., Heyrovsky sq. 2, 162 06 Prague, Czech Republic. E-mail: rodriguez@imc.cas.cz; Fax: +420 296 809 410; Tel: +420 296 809 333.

[b] Cellular Microbiology and Physics of Infection Group, CNRS UMR 8204, INSERM U1019, Institut Pasteur de Lille, Lille University, Lille, France.

[c] Institute for Applied Materials (IAM), Karlsruhe Nano Micro Facility (KNMF), Karlsruhe Institute of Technology (KIT), Hermann-von-Helmholtz-Platz 1, 76344 Eggenstein-Leopoldshafen, Germany

† Electronic Supplementary Information (ESI) available: Materials, synthesis of the silane-ATRP-initiator, synthesis of monomers, additional methods of characterisation (ellipsometry, contact angle, XPS, SPR), preparation of the colloidal probe cantilever, detailed chemical characterisation of the initiator layer and polymer brushes by XPS, AFM topography images, protein fouling, and confirmation of the cell viability after screening. See DOI: 10.1039/b000000x/

1. J. W. Costerton, P. S. Stewart and E. P. Greenberg, *Science*, 1999, **284**, 1318-1322.
2. P. Kingshott, J. Wei, D. Bagge-Ravn, N. Gadegaard and L. Gram, *Langmuir*, 2003, **19**, 6912-6921.
3. R. O. Darouiche, *New England Journal of Medicine*, 2004, **350**, 1422-1429.
4. D. J. Stickler, *Current Opinion in Infectious Diseases*, 2000, **13**, 389-393.
5. J. Hasan, R. J. Crawford and E. P. Ivanova, *Trends Biotechnol.*, 2013, **31**, 295-304.
6. S. J. Yuan, S. O. Pehkonen, Y. P. Ting, K. G. Neoh and E. T. Kang, *Langmuir*, 2010, **26**, 6728-6736.
7. H. J. Busscher and H. C. van der Mei, *PLoS Pathog*, 2012, **8**, e1002440.
8. M. Y. Wu, V. Sendamangalam, Z. Xue and Y. Seo, *Biofouling*, 2012, **28**, 1119-1128.
9. B. Schachter, *Nat Biotech*, 2003, **21**, 361-365.
10. H. Ceri, M. E. Olson, C. Stremick, R. R. Read, D. Morck and A. Buret, *J. Clin. Microbiol.*, 1999, **37**, 1771-1776.
11. M. E. Davey and G. A. O'Toole, *Microbiology and Molecular Biology Reviews*, 2000, **64**, 847-867.
12. O. Rzhepishevska, S. Hakobyan, R. Ruhal, J. Gautrot, D. Barbero and M. Ramstedt, *Biomaterials Science*, 2013, **1**, 589-602.
13. X. Laloyaux, E. Fautré, T. Blin, V. Purohit, J. Leprince, T. Jouenne, A. M. Jonas and K. Glinel, *Adv. Mater.*, 2010, **22**, 5024-5028.
14. K. Glinel, A. M. Jonas, T. Jouenne, J. r. m. Leprince, L. Galas and W. T. S. Huck, *Bioconjugate Chem.*, 2008, **20**, 71-77.

15. S. H. Hakobyan, O. Rzhepishevska, R. Ruhal and M. Ramstedt, *European Cells and Materials*, 2013, **26**, 37.
16. M. Krishnamoorthy, S. Hakobyan, M. Ramstedt and J. E. Gautrot, *Chem. Rev.*, 2014, **114**, 10976-11026.
17. F. Hui and C. Debiemme-Chouvy, *Biomacromolecules*, 2013, **14**, 585-601.
18. W. J. Yang, T. Cai, K. G. Neoh, E. T. Kang, G. H. Dickinson, S. L. Teo and D. Rittschof, *Langmuir*, 2011, **27**, 7065-7076.
19. R. Wang, K. G. Neoh, Z. Shi, E. T. Kang, P. A. Tambyah and E. Chiong, *Biotechnol. Bioeng.*, 2012, **109**, 336-345.
20. R. Hu, G. Li, Y. Jiang, Y. Zhang, J.-J. Zou, L. Wang and X. Zhang, *Langmuir*, 2013, **29**, 3773-3779.
21. Y. Wang, E. Y. Chi, D. O. Natvig, K. S. Schanze and D. G. Whitten, *ACS Applied Materials & Interfaces*, 2013, DOI: 10.1021/am400220s.
22. G. Gao, D. Lange, K. Hilpert, J. Kindrachuk, Y. Zou, J. T. J. Cheng, M. Kazemzadeh-Narbat, K. Yu, R. Wang, S. K. Straus, D. E. Brooks, B. H. Chew, R. E. W. Hancock and J. N. Kizhakkedathu, *Biomaterials*, 2011, **32**, 3899-3909.
23. M. Ramstedt, N. Cheng, O. Azzaroni, D. Mossialos, H. J. Mathieu and W. T. Huck, *Langmuir*, 2007, **23**, 3314-3321.
24. G. Cheng, H. Xue, Z. Zhang, S. Chen and S. Jiang, *Angew. Chem. Int. Ed.*, 2008, **47**, 8831-8834.
25. M. Ramstedt, B. Ekstrand-Hammarstrom, A. V. Shchukarev, A. Bucht, L. Osterlund, M. Welch and W. T. Huck, *Biomaterials*, 2009, **30**, 1524-1531.
26. C. Rodriguez-Emmenegger, M. Houska, A. B. Alles and E. Brynda, *Macromol. Biosci.*, 2012, **12**, 1413-1422.
27. C. Rodriguez-Emmenegger, E. Brynda, T. Riedel, M. Houska, V. Šubr, A. Bologna Alles, E. Hasan, J. E. Gautrot and W. T. S. Huck, *Macromol. Rapid Commun.*, 2011, **32**, 952–957.
28. C. Rodriguez-Emmenegger, E. Brynda, T. Riedel, Z. Sedlakova, M. Houska and A. B. Alles, *Langmuir*, 2009, **25**, 6328-6333.
29. A. Clements, F. Gaboriaud, J. F. Duval, J. L. Farn, A. W. Jenney, T. Lithgow, O. L. Wijburg, E. L. Hartland and R. A. Strugnell, *PLoS ONE*, 2008, **3**, e3817.
30. R. Bos, H. C. van der Mei and H. J. Busscher, *FEMS Microbiology Reviews*, 1999, **23**, 179-230.
31. Y. Chen, A. K. Harapanahalli, H. J. Busscher, W. Norde and H. C. van der Mei, *Applied and Environmental Microbiology*, 2014, **80**, 637-643.
32. A. Roosjen, H. J. Busscher, W. Norde and H. C. van der Mei, *Microbiology*, 2006, **152**, 2673-2682.
33. C. J. Van Oss, M. K. Chaudhury and R. J. Good, *Chem. Rev.*, 1988, **88**, 927-941.
34. H. J. Kaper, H. J. Busscher and W. Norde, *Journal of Biomaterials Science -- Polymer Edition*, 2003, **14**, 313-324.
35. F. Boulmedais, B. Frisch, O. Etienne, P. Lavalle, C. Picart, J. Ogier, J. C. Voegel, P. Schaaf and C. Egles, *Biomaterials*, 2004, **25**, 2003-2011.
36. E. Ostuni, R. G. Chapman, M. N. Liang, G. Meluleni, G. Pier, D. E. Ingber and G. M. Whitesides, *Langmuir*, 2001, **17**, 6336-6343.
37. B. Zdyrko, V. Klep and I. Luzinov, *Langmuir*, 2003, **19**, 10179-10187.
38. A. Halperin, G. Fragneto, A. Schollier and M. Sferrazza, *Langmuir*, 2007, **23**, 10603-10617.
39. A. Halperin, *Langmuir*, 1999, **15**, 2525-2533.
40. S. I. Jeon, J. H. Lee, J. D. Andrade and P. G. De Gennes, *J. Colloid Interface Sci.*, 1991, **142**, 149-158.
41. A. de los Santos Pereira, T. Riedel, E. Brynda and C. Rodriguez-Emmenegger, *Sens. Actuators, B*, 2014, **202**, 1313-1321.
42. D. Leckband, S. Sheth and A. Halperin, *Journal of Biomaterials Science-Polymer Edition*, 1999, **10**, 1125-1147.
43. R. C. Advincula, 2006, **197**, 107-136.
44. M. Zamfir, C. Rodriguez-Emmenegger, S. Bauer, L. Barner, A. Rosenhahn and C. Barner-Kowollik, *J. Mater. Chem. B*, 2013, **1**, 6027-6034.
45. T. Tischer, C. Rodriguez-Emmenegger, V. Trouillet, A. Welle, V. Schueler, J. O. Mueller, A. S. Goldmann, E. Brynda and C. Barner-Kowollik, *Adv. Mater.*, 2014, **26**, 4087-4092.
46. F. Surman, T. Riedel, M. Bruns, N. Y. Kostina, Z. Sedláková and C. Rodriguez-Emmenegger, *Macromol. Biosci.*, 2015, **10.1002/mabi.201400470**.
47. A. de los Santos Pereira, C. Rodriguez-Emmenegger, F. Surman, T. Riedel, A. Bologna and E. Brynda, *RSC Advances*, 2014, **4**, 2318 - 2321.
48. G. Cheng, Z. Zhang, S. Chen, J. D. Bryers and S. Jiang, *Biomaterials*, 2007, **28**, 4192-4199.
49. C. Rodriguez-Emmenegger, A. Decker, F. Surman, C. M. Preuss, Z. Sedláková, N. Zydziak, C. Barner-Kowollik, T. Schwartz and L. Barner, *RSC Adv.*, 2014, **4**, 64781-64790.
50. J. Helenius, C. P. Heisenberg, H. E. Gaub and D. J. Muller, *J. Cell Sci.*, 2008, **121**, 1785-1791.
51. F. Mosconi, J. F. Allemand and V. Croquette, *Rev. Sci. Instrum.*, 2011, **82**, 034302.
52. E. Evans, K. Ritchie and R. Merkel, *Biophys. J.*, 1995, **68**, 2580-2587.
53. A. L. Rutz, K. E. Hyland, A. E. Jakus, W. R. Burghardt and R. N. Shah, *Adv. Mater.*, 2015, DOI: 10.1002/adma.201405076, n/a-n/a.
54. A. Beaussart, S. El-Kirat-Chatel, P. Herman, D. Alsteens, J. Mahillon, P. Hols and Y. F. Dufrene, *Biophys. J.*, 2013, **104**, 1886-1892.
55. A. Beaussart, P. Herman, S. El-Kirat-Chatel, P. N. Lipke, S. Kucharikova, P. Van Dijck and Y. F. Dufrene, *Nanoscale*, 2013, **5**, 10894-10900.
56. G. Zeng, T. Müller and R. L. Meyer, *Langmuir*, 2014, **30**, 4019-4025.
57. O. Guillaume-Gentil, E. Potthoff, D. Ossola, C. M. Franz, T. Zambelli and J. A. Vorholt, *Trends Biotechnol.*, 2014, **32**, 381-388.
58. M. Benoit, D. Gabriel, G. Gerisch and H. E. Gaub, *Nature Cell Biology*, 2000, **2**, 313-317.
59. C. Blaszykowski, S. Sheikh and M. Thompson, *Chem. Soc. Rev.*, 2012, **41**, 5599-5612.
60. A. de los Santos Pereira, T. Riedel, E. Brynda and C. Rodriguez-Emmenegger, *Sensors and Actuators B: Chemical*, 2014, **202**, 1313-1321.
61. C. Rodriguez-Emmenegger, E. Brynda, T. Riedel, Z. Sedlakova, M. Houska and A. Bologna Alles, *Langmuir*, 2009, **25**, 6328-6333.
62. S. Edmondson, N. T. Nguyen, A. L. Lewis and S. P. Armes, *Langmuir*, 2010, **26**, 7216-7226.
63. N. Cheng, A. A. Brown, O. Azzaroni and W. T. S. Huck, *Macromolecules*, 2008, **41**, 6317-6321.
64. C. Rodriguez-Emmenegger, E. Hasan, O. Pop-Georgievski, M. Houska, E. Brynda and A. Bologna Alles, *Macromolecular Bioscience*, 2012, **12**, 525-532.
65. C. Pujol and J. B. Bliska, *Infection and Immunity*, 2003, **71**, 5892-5899.
66. M. Krzywinski and N. Altman, *Nature Methods*, 2014, **11**, 119-120.
67. C. Rodriguez-Emmenegger, E. Hasan, O. Pop-Georgievski, M. Houska, E. Brynda and A. Bologna Alles, *Macromol. Biosci.*, 2011, **12**, 525-532.
68. C. Rodriguez-Emmenegger, O. A. Avramenko, E. Brynda, J. Skvor and A. Bologna Alles, *Biosens. Bioelectron.*, 2011, **26**, 4545-4551.
69. S. Gon, K. N. Kumar, K. Nusslein and M. M. Santore, *Macromolecules*, 2012, **45**, 8373-8381.
70. T. Riedel, C. Rodriguez-Emmenegger, A. de los Santos Pereira, A. Bědajánková, P. Jinoch, P. M. Boltovets and E. Brynda, *Biosens. Bioelectron.*, 2014, **55**, 278-284.
71. K. Rechendorff, M. B. Hovgaard, M. Foss, V. P. Zhdanov and F. Besenbacher, *Langmuir*, 2006, **22**, 10885-10888.
72. A. E. Nel, L. Madler, D. Velegol, T. Xia, E. M. V. Hoek, P. Somasundaran, F. Klaessig, V. Castranova and M. Thompson, *Nature Materials*, 2009, **8**, 543-557.
73. A. Jain and N. B. Bhosle, *Biofouling*, 2009, **25**, 13-19.
74. C. Tedjo, K. G. Neoh, E. T. Kang, N. Fang and V. Chan, *J Biomed Mater Res A*, 2007, **82**, 479-491.
75. G. Hwang, S. Kang, M. G. El-Din and Y. Liu, *Biofouling*, 2012, **28**, 525-538.
76. V. Dupres, C. Verbelen, D. Raze, F. Lafont and Y. F. Dufrêne, *ChemPhysChem*, 2009, **10**, 1672-1675.

77. A. Beaussart, S. El-Kirat-Chatel, R. M. A. Sullan, D. Alsteens, P. Herman, S. Derclaye and Y. F. Dufrêne, *Nat. Protocols*, 2014, **9**, 1049-1055.
78. O. Pop-Georgievski, C. Rodriguez-Emmenegger, A. de los Santos Pereira, V. Proks, E. Brynda and F. Rypacek, *J. Mater. Chem. B*, 2013, **1**, 2859-2867.
79. H. Dermutz, R. R. Gruter, A. M. Truong, L. Demko, J. Voros and T. Zambelli, *Langmuir*, 2014, **30**, 7037-7046.
80. G. Zeng, T. Muller and R. L. Meyer, *Langmuir*, 2014, **30**, 4019-4025.
81. Q. Shao, A. D. White and S. Jiang, *The Journal of Physical Chemistry B*, 2013, **118**, 189-194.
82. Y. El Tahir and M. Skurnik, *International Journal of Medical Microbiology*, 2001, **291**, 209-218.
83. S. Jiang and Z. Cao, *Adv. Mater.*, 2010, **22**, 920-932.
84. J. Wu, W. Lin, Z. Wang, S. Chen and Y. Chang, *Langmuir*, 2012, DOI: 10.1021/la300394c.
85. C. Leng, X. Han, Q. Shao, Y. Zhu, Y. Li, S. Jiang and Z. Chen, *The Journal of Physical Chemistry C*, 2014, **118**, 15840-15845.

